

Incorporating Demand Dynamics in Multi-Period Capacitated Fast-Charging Location Planning for Electric Vehicles

Anpeng Zhang[†], Jee Eun Kang[†], and Changhyun Kwon^{*‡}

[†]Department of Industrial and Systems Engineering, University at Buffalo, SUNY

[‡]Department of Industrial and Management Systems Engineering, University of South Florida

April 27, 2017

Abstract

We develop a multi-period capacitated flow refueling location problem for electric vehicles (EVs) as the EV market responds to the charging infrastructure. The optimization model will help us determine the optimal location of level 3 chargers as well as the number of charging modules at each station over multiple time periods. Our model can also be applied to fast-filling gaseous alternative fuel vehicles under similar assumptions. We define a number of demand dynamics, including flow demand growth as a function of charging opportunities on path as well as natural demand growth independent of charging infrastructure. We also present an alternative objective function of maximizing electric vehicle demand in addition to maximizing flow coverage. A case study based on a road network around Washington, D.C., New York City, and Boston is presented to provide numerical experiments related to demand dynamics, showing the potential problems in multi-period planning.

Keywords: electric vehicles; facility location; flow refueling location problem; multi-period planning; vehicle market demand dynamics; alternative fuel vehicles

1 Introduction

Recently, alternative fuel vehicles (AFV) are gaining attention worldwide due to growing concerns of environmental problems. Different types of fuel including electricity, natural gas and hydrogen try to take place of petroleum to reduce the greenhouse and other emissions. However, the refueling facility network for AFVs is not as mature as that of conventional gas stations and is not widely distributed. The deficiency of charging stations has been mentioned as one of the barriers that prevent AFVs from becoming more popular in several studies (Melaina, 2003; Kuby and Lim, 2005, 2007; Melaina and Bremson, 2008; Shukla et al., 2011; Chung and Kwon, 2015). A better network of charging service would improve the use of electric vehicles (EV), and more EV users would promote

*Corresponding author; chkwon@usf.edu

the construction of infrastructure. Another barrier for promoting AFVs is the limited vehicle range (Shukla et al., 2011; Wang and Lin, 2009; Wang and Wang, 2010; Lim and Kuby, 2010; Capar and Kuby, 2012; Romm, 2006; Chung and Kwon, 2015). While the coming generation of luxury EVs should have ranges much higher than 160 km, most of the EVs currently have a range of 60 km to 160 km with full battery. Thus, the current EV range may not be sufficient for long distance intercity trips. Due to these limits, building a charging network and choosing the right locations for chargers is helpful to popularize the use of EVs and solve the environmental problems caused by conventional vehicles.

These facts motivate the need of the study on optimal locations for refueling or charging stations in networks with different sizes. Thus, several models for optimal location of alternative-fuel stations are developed to solve this problem. Two popular models are the p -median and flow-refueling models. The p -median model locates a set of facilities to cover all the demands at the nodes of the network while minimizing the total traveled distance from each demand node to the facilities. Nicholas and Ogden (2006) worked on the applications in AFVs with p -median models. Similarly, the p -center location model is a minimax problem that locates p facilities to minimize the maximum distance from any demand node to its closest facility (Hakimi, 1964, 1965; Minieka, 1970; Suzuki and Drezner, 1996; Drezner, 1984). Also, the set cover model minimizes the number or cost of facilities needed to cover all demand nodes within a specific distance (Toregas et al., 1971). In addition, there are diverse models with different assumptions that the travel demands occur at facilities on paths, including convenient stores, gasoline stations and fast-food restaurants. The flow-capturing location model (FCLM) locates p facilities to capture the origin-destination flow, and travel demands are served by facilities located at nodes on the paths (Hodgson, 1990; Berman et al., 1992). Later, flow-refueling location problem (FRLM) enhance the model by cover the flow on a path with a combination of facilities, instead of one facility in FCLM, based on the assumption of the limited range of AFVs.

In this paper, we focus on modeling for EVs and charging stations. Our model aims to find optimal solution for the construction planning of level 3 or fast charging stations along highways, and we assume home charging has little effect on the planning decisions. For level 1 or level 2 charging stations, the full-charging time greatly depends on the remaining battery level of the vehicle and the station location is affected by the starting battery level. In addition, vehicles rarely recharge at level 1 or level 2 charging stations mid-route since the charging time is too long. Thus our model fits less well for slow charging facilities due to our current assumptions. (See Section 3.1) We, however, note that this model is general and applicable for other types of AFV refueling network planning. The capacity constraint in our model is based on the fact that limited EVs can be served in unit time. Capacity constraint can also be extended to refueling facilities for single-fuel vehicles that use liquid or gaseous fuels, such as H₂ and CNG, since the amount of fuel available at each facility is limited. Our model applies well to those AFVs that refueled quickly in about the same amount of time regardless of tank level, given people rarely refuel those AFVs at home. Our extension is based on FRLM while considering facility capacity and infrastructure planning

time. First, facility capacity, or charging times of EVs, should be included in the model. Different from conventional vehicles or other AFVs, EVs could take 2-8 hours to be fully charged on Level 1 or 2 charging stations. Even on Level 3 charging stations, drivers may have to wait for 20 to 30 minutes to charge their vehicles. Thus, the number of vehicles that can be served at one charging facility in unit time is limited, which could be considered as the capacity of the facilities. Also, the “uncapacitated” assumption in FRLM is based on the limited number of early users of AFVs, and one facility might satisfy all of the demand. With the increasing market share of EVs, it’s less realistic to serve all of travel demands with one facility in the near future. Second, we consider the multi-period model since it usually takes a long time to plan and build a charging network with sufficient facilities. The facility location decision involves many factors, including investment and policy, and these factors might vary from time to time. In addition, the infrastructure should be compatible to the number of AFV users so the planner is more likely to finish the whole charging network in several time stages. Thus, a strategic multi-period infrastructure plan is more helpful to the decision maker.

We incorporate EV demand dynamics to multi-period capacitated flow refueling station planning, realizing the importance of charging availability in EV demand. Charging network (or charging availability) affects EV demand and the growth of the demand affects planning decisions. By incorporating demand dynamics in multi-period planning, we capture the effects of station siting decisions on future demand and this allows us to observe this interaction between demand and supply. In addition, we would also like to see how planning decisions will be reacting to different demand dynamics, as well as different objectives of station siting.

We introduce different travel demands (total vehicle flow and EV flow). The number of all vehicles, including conventional vehicle and AFVs, going from a location (origin) to another location (destination) in the network is referred to as the *total vehicle flow* of the OD pair, while the corresponding number of electric vehicles are referred as the *EV flow*. The proportion of electric vehicles in total vehicles is denoted as the *EV market share*. The amount of EV flow is naturally the *EV demand*, and market share is directly observed from these two demands. The concept of *demand dynamics* is to provide different scenarios on how vehicle demand changes with time and user’s decisions.

The remainder of this paper is organized as follows. In Section 2, we review the arc-cover-path cover formulation of FRLM, as well as the related research. In Section 3, we describe our problem and provide the formulation of our multi-period capacity model as well as the demand dynamics of EV. In Section 4, we present our heuristic method to solve the model, and utilize line search method to improve our computational efficiency. In Section 5, we present extensive computational results for the highway network for the region between Washington DC and Boston. Diverse scenarios with different demand dynamics and objectives are tested to evaluate model performance, and to provide help for policy makers. Numerical results of the influence of time periods in multi-period planning are also provided. Section 6 concludes the paper by listing the suggestions to policy makers and by providing directions for future research.

2 Literature Review

Hodgson (1990) and Berman et al. (1992) developed the flow-capturing location model (FCLM), a flow-intercepting model to help locate retail facilities such as convenient stores, banking machines and billboards. Different from traditional node-based models that express demand as a weight at nodes, FCLM considered the traffic flow between OD pairs and locate p facilities to maximize the traffic flow “captured.” In FCLM, the flow is captured if a facility is built on the shortest path between its origin and its destination. These models are path-based models as they relate traffic flow demand with the path and “capture” them with the facilities along the path.

Kuby and Lim (2005) later extended FCLM to the flow-refueling location model (FRLM) to identify locations of AFV refueling facilities while considering the limited traveling range of AFVs. Different from FCLM, the vehicle in the traffic flow could refuel at several facilities if needed. If the vehicle could reach its destination and go back to its origin along the shortest path without using up fuel, the traffic flow between the OD pair was considered refueled. Since all flows had to be covered regardless of demand, they used only a node-to-node distance matrix as their input without information of OD demand. FRLM was also a path-based model, and several facilities might be required to refuel a flow. This required a pre-generation of valid facility combinations on each path, and the model could be hard to solve in large networks.

New formulations and extensions were developed to improve efficiency, reliability or flexibility. Upchurch et al. (2009) included facility capacity considerations and reduced the number of constraints in their capacity-FRLM (CFRLM) by eliminating the intermediate role of the combination variable. With consideration of the remaining fuel of each vehicle at each node of all paths, Wang and Lin (2009) introduced a new formulation of FRLM following the concept of set covering while pre-generation of facility combinations was not required. They used only distance matrix as their input, which then considered network topology without information of OD demand. Wang and Wang (2010) extended Wang and Lin (2009)’s model to consider nodal demands, and they provided a dual objective model by adding an objective function to maximize the flow coverage. Wang and Lin (2013) provided a capacitated extension based on Wang and Lin (2009)’s model considering multiple type of charging stations, constrained facility budget and vehicle routing behavior. Lim and Kuby (2010) proposed heuristic algorithms to solve larger problems as they showed the pre-processing stage of FRLM is quite time-consuming. Capar and Kuby (2012) presented a new MIP formulation which did not require generating facility combinations and could be applied in larger networks. While their model needed more variables and constraints, Capar and Kuby (2012) introduced a new formulation of FRLM with high efficiency and flexibility with a network expansion method. In their model, the process of generating valid facility combinations was no longer needed, which greatly reduced the time to solve either set-covering or maximum coverage problem in large scale networks. By constructing an expanded network, MirHassani and Ebrazi (2012) provided a new formulation of FRLM with both set-covering form and maximum coverage form without pre-generation process requirement. In set-covering form, their model would ensure all demand are covered with lowest cost. In maximum coverage form, their model would maximize the total flow coverage with fixed

Table 1: Notation for AC-PC (1)–(4)

N	Set for all the nodes in the network
Q	Set of OD pairs
q	the index for OD pairs (and the path between them)
p	Number of facilities to be located
$a_{j,k}$	a directional arc from node j to node k
A^q	Set of directional arcs on path q , sorted from origin to destination and back to origin
K_{jk}^q	Set of candidate nodes that can refuel $a_{j,k}$ in A^q
f_q	Volume of traffic flow on path q
y_q	Binary variable, equals to unity if the flow on path q is covered
z_i	Binary variable, equals to unity if a station is built at site i

number of facilities.

Later, Capar et al. (2013) provided an arc cover-path cover model (AC-PC) as a new formulation of FRLM, based on the idea of covering each arc from all paths. They introduced a new candidate set in their new formulation so that they could improve computational efficiency significantly by skipping the pre-generation process. With the notation in Table 1, the formulation of AC-PC model is as follows:

$$\max \sum_{q \in Q} f_q y_q \quad (1)$$

subject to:

$$\sum_{i \in K_{jk}^q} z_i \geq y_q \quad \forall q \in Q, a_{jk} \in A^q \quad (2)$$

$$\sum_i z_i = p \quad (3)$$

$$y_q, z_i \in \{0, 1\} \quad \forall q \in Q, i \in N \quad (4)$$

The AC-PC model located p facilities to maximize the total traffic flow refueled. The key constraint (2) makes sure that each arc on the path can be refueled at one of the open facilities, and the flow on the path is refueled if all the arcs on the path are travelable. In this formulation, each arc on the path provides one constraint, and all the arcs on the same path together decide if the flow on the path is refueled. Thus, the pre-generation of facility combinations is eliminated, and the candidate set K_{jk}^q , becomes the key of the model.

In the following part, we will explain how to generate the candidate set. Suppose we have a path with n nodes. The first node is the origin and the n -th node is the destination. For each arc, we will generate one candidate set. Check all the nodes on the path with the following rules.

For arc from node j to node k ($j < k$), the i -th node on the path is in the candidate set:

1. If $i \leq j$ and the distance between i and k , denoted as $d(i, k)$, is within vehicle range.

Table 2: Notation for CFRLM (5)

Q	Set of OD pairs
q	the index for OD pairs (and the path between them)
f_q	Volume of traffic flow on path q
k	Index of potential facility location
K	Set of all potential facility locations
h	Index of combinations of facilities
b_{qh}	Equal to 1 if facility combination h can refuel path q , otherwise equal to 0
y_{qh}	Proportion of f_q being refueled by facility combination h
e_q	the fraction of round trips on average that requires refueling
g_{qhk}	Average number of times for a vehicle on path q to stop and refuel at facility k in combination h
c	Number of vehicle stops that can be refueled by each module
x_k	Number of modules at location k

2. If $i \geq k$ and $d(1, i) + D(1, k)$ is within vehicle range.

For arc from k to j ($j < k$), the i -th node on the path is in the candidate set:

1. If $i \leq j$ and $d(i, n) + d(j, n)$ is within vehicle range.
2. If $i \geq k$ and $d(j, i)$ is within vehicle range.

In addition to the original FRLM, we are also interested in the facility capacity as well as the multi-period planning. Motivated by the increasing number of AFVs that may appear in the future, Upchurch et al. (2009) provided a new formulation of FRLM with consideration of facility capacity, namely Capacitated FRLM (CFRLM), trying to handle the increasing demand in a more realistic way. In their CFRLM formulation, capacity was defined in interchangeable modular units, and the amount of flow travel through the facility was limited, indicated by a linear variable. A capacity constraint, based on those in capacitated fixed-charge location problems (Sa, 1969; Davis and Ray, 1969), was added in the model. With the notation in Table 2, the capacity constraint can be written as follows:

$$\sum_{q \in Q} \sum_{h | b_{qh}=1} e_q g_{qhk} f_q y_{qh} \leq c x_k \quad \forall k \in K \quad (5)$$

where the left hand side sums the use of the facilities and combinations of facilities for each flow, and the right hand side is the total facility capacity built. A similar idea is implemented in our model, making sure that the flow passing through the charging station does not exceed its capacity. As we focus on building Level 3 stations, the “fuel” of our stations is electricity transmitted by wire and our main limit is the charging time for electric vehicles. In other words, each facility can only

serve a limited number of vehicles in unit time, which is our definition of facility capacity. Therefore, the capacity constraint in our model is the limit on the number of vehicles being able to pass the recharging station in a certain amount of time.

To make the charging network more realistic, Chung and Kwon (2015) focused on multi-period infrastructure planning. Their paper mentioned that the authority responsible for the construction of the charging network might not invest due to the limited number of early triers of electric vehicles, and thus could not attract potential consumers. However, a strategic infrastructure plan might help guarantee the future of electric vehicles for buyers and alleviate the economic pressure for the authority. Motivated by the need of multi-period planning, Chung and Kwon (2015) provided a multi-period optimization method by extending FRLM, a Forward myopic (F-myopic) method and a Backward myopic (B-myopic) method. The ideas are similar in this paper that multi-period model tries to optimize the whole plan for all time periods, while myopic methods only solve a single-period model for each time period successively. Comparing to myopic methods, the multi-period optimum (M-opt) model is more computational resource consuming in large networks. In most cases, B-myopic method is able to provide an acceptable result, though this could be affected by the distribution of travel demand.

Recently, Arslan and Karaşan (2016) extend the FRLM by considering charging stations for multiple types of plug-in hybrid electric vehicles with different ranges while minimizing the total cost of transportation under the existing cost structure between gasoline and electricity. In addition to the conventional models based on FRLM, Strehler et al. (2017) present a constrained shortest path problem for the routing of electric and hybrid vehicles with convertible resources and charging stations while Liao et al. (2016) solve similar routing based problem considering both vehicle loading capacities and charging stations. Hof et al. (2017) focus on the electric vehicle routing problems (E-VRPs) to solve the battery swap station location-routing problem with capacitated electric vehicles, and Montoya et al. (2017) extend the E-VRP models to consider nonlinear charging functions. Different from choosing the optimal location for fixed charging stations, Chen et al. (2016) develop a new user equilibrium model to optimize the deployment plan of charging lanes. Multiple types of charging stations as well as wireless charging technology are also considered in Liu and Wang (2017), and they provide optimal location of multiple types of BEV recharging facilities while minimizing the public social cost. Xu et al. (2017b) develop a mixed logit model to study the influence of BEV users' choice of charging mode and location to find optimal public charging station locations as well as strategy for power peak-load shifting. Some other recent studies also focus on strategic or operational decision-makings to popularize BEVs considering touring, fleet deployment, network equilibrium problem, shared mobility and etc (Nie et al., 2016; Fetene et al., 2016; Liao et al., 2016; Boyacı et al., 2017; Xu et al., 2017a).

Despite the advances made in the adoption of EVs, the demand dynamics and growth have been largely ignored in the literature related to FRLM and other station siting problems. On the other hand, refueling/recharging station infrastructure (also often referred as charging network) has been consistently identified as a key factor in AFV purchase decisions along with factors such as cost,

range, environmental benefit, etc. (Brownstone et al., 1996; Ewing and Sarigöllü, 2000; Dagsvik et al., 2002; Hidrue et al., 2011; Ahn et al., 2008; Liu and Greene, 2012). Some simulation studies also confirmed that both *demand dynamics* and *placement of refueling stations* were key factors of overcoming the “chicken-and-egg” problem of AFV demand and infrastructure and for these AFVs to successfully survive in the market. Agent based models has been developed to simulate the behaviors of hydrogen fuel suppliers and vehicle owners. Stephan and Sullivan (2004) applied this model in a square urban area to test a hydrogen-based personal transportation system as well as the initial placement of stations. They made two behavior assumptions, and tested them with this model. Drivers were more likely to buy a hydrogen vehicle with higher refueling opportunity on their trips, while hydrogen fuel suppliers would add more hydrogen pumps if there are more hydrogen vehicles on the trip. Schwoon (2007) made similar assumptions that consumers were more likely to buy a fuel cell vehicle if they experienced more hydrogen refueling opportunities on trips of long distance. In their work, they integrated the agent-based model and geographic information system as a tool to test the potential success of several initial hydrogen outlets distributions in the German trunk road system. They concluded that drivers’ worry factor on refueling opportunities can determine the optimal initial distribution of refueling stations, and the initial placement was the key factor of AFVs’ surviving.

In this paper, we incorporate demand dynamics to the multi-period capacitated flow-refueling location model. We define introduce a term, the fraction of EVs on each Origin-Destination travel demand, within the FRLM. Then a number of demand dynamics are defined quantify the dynamics of EV travel demand and charging availability. We develop a heuristic method utilizing line search method to solve the model in large scale networks.

3 The Model

3.1 Multi-Period Planning Problem Description

We consider the multi-period flow refueling location problem with capacity constraints and demand dynamics. Our problem aims to identify charging locations and the numbers of charging modules to build in each time period, so that the total flow covered in all time periods is maximized. The station locations decide where vehicles can be charged, and more modules are able to provide service for more vehicles at the same time. Single time period capacitated AC-PC model is a special case of our general multi-period model.

The assumptions of the proposed model are similar to the common assumptions in the models of FRLM and its variations (Hodgson, 1990; Kuby and Lim, 2005; Zeng et al., 2010; Capar and Kuby, 2012; Capar et al., 2013). In this paper, the interpretation of the concept of *capacity* is defined for EVs. For fast refueling stations with different fuel, the facility capacity can be related to the size of the underground tank, the frequency of delivery, the number of pumps or other relevant limits depending on different technologies. For instance, some stations produce their own H₂, then the capacity could be the daily amount of H₂ that the electrolyzer or steam methane reformer can

generate. Since different technologies have various limitations, we can apply different definition on the capacity variable c such as fixed value or flexible functions when applying our model to various types of AFVs. For EVs, chargers are usually connected to the grid, and they have no fuel tank limit such as petroleum or hydrogen. On the other hand, EVs take longer to be charged compared to refueling fuel-type vehicles. Thus, the number of vehicles that can be served by each charger in unit time is limited. This is the serving capacity for each EV charger. In addition, we assume our infrastructure decisions will affect the EV demand, resulting in the user's decision and EV market share on each path, which will reversely affect planning decisions in future. We make the following assumptions:

1. The traffic flows through the shortest path and drivers stop to recharge along the way;
2. The total demand between OD pairs are given;
3. Drivers will charge the battery to full level as they need, and they know the location of charging stations;
4. Only nodes of the network are considered as locations of recharging stations;
5. Vehicles have constant driving ranges;
6. Battery level declines linearly with distance traveled;
7. Vehicles start with at least half-full battery;
8. Only passenger automobile vehicles are considered, motor cycles or trucks are not included;
9. Charging a vehicle to full battery level takes the constant amount of time;
10. Only the market share of the total traffic flow on each path is considered in the model;
11. The EV market share in the current time period is related to the network flow coverage and the EV market share in the previous time period;

Also, a traffic flow is considered as *served* if an EV can start from origin, travel to destination, and come back to origin without running out of battery. In this paper, we assume that level 1 and level 2 slow charging is not done since we are considering long-distance and highway-only network. The starting battery level is related to recharging station locations, being full with station at origin or being the remaining electricity power from the last recharging on the same path. For the above assumption 7, it could be more realistic to assume vehicles start the trip with full-battery level considering home charging for EVs. EVs such as the Nissan Leaf with smaller batteries are usually fully charged in hours while new EV models with larger battery might not be fully charged overnight at home. Thus, we are not assuming full-battery level for now to be consistent with the assumptions of AC-PC model (Capar et al., 2013) where AFVs start the trips with at least half tank of fuel. In addition, some travelers might start the trip from home just after finishing another trip, leaving

insufficient time for EVs to be fully charged. Also, the origin of the trips might not be home in real case studies, such as highway entrances in our case study; other AFVs using H2 and CNG which are generally not filled at home also support our assumption 7; thus we assume that the vehicles starts with at least half full battery without losing generality. For the above assumption 9, the remaining power in the battery will not affect the time of recharging battery to full level in order to simplify the problem. In other words, filling a vehicles tank or battery uses a constant (average) increment of station capacity. In reality, time needed to charge electric vehicle to full battery is related to the remaining energy in battery as well as the charging rate of facility in most cases. However, the assumption is reasonable for fast-charging of EVs, such as Tesla superchargers and the coming European luxury competitors, since recharging takes about the same amount of time. Our assumption 9 is also suited for single-fuel vehicles that use liquid or gaseous fuels given refueling events are finished quickly in about the same amount of time regardless of tank level. However, the varying charging time would make the problem more complicated. Thus, we make the assumption of constant charging time so that the capacity of facility can be simplified to the number of charging times, which is consistent with CFRLM from Upchurch et al. (2009). This less realistic assumption is a simplification in the initial model, and more realistic assumptions could be applied in future work. With our current assumptions, our model is also well suited for single-fuel vehicles that use liquid or gaseous fuels in addition to the fast-charging EVs with large battery in our case study.

3.2 Demand Dynamics of EV

We incorporate the EV demand in the multi-period planning problem with demand dynamics. In multi-period planning, the number of stations and modules (charging network and opportunity) will influence the demand in future time periods. Despite the evidence that charging opportunities (charging network) will influence EV purchase decision and therefore overall market share (Brownstone et al., 1996; Ewing and Sarigöllü, 2000; Dagsvik et al., 2002; Hidrue et al., 2011; Ahn et al., 2008; Liu and Greene, 2012), there has been little understanding how these market share will translate to EV travel demand share instead. That is, it is unclear how early EV adopters will utilize their vehicles, represented by travel demand, which is represented with flow on path, f_q in FRLM literature. We present a number of demand dynamics between charging availability and EV share of travel demand; the EV share of travel demand for path q at time t is defined as s_q^t . The overall market share will be an average value, $\frac{1}{|Q|} \sum_{q \in Q} s_q^t$.

Now, we assume that the EV market share on each path in the current time period is related to the previous time period's EV market share, EV flow coverage on the path in the previous time period as well as natural market growth. Thus, we use a flexible function $\Delta(\cdot)$ to simulate different demand dynamics in the following equation of EV market share. Flow coverage will be EV flow coverage in the following sections if there are no specific explanations.

$$s_q^t = \Delta(\varepsilon, s_q^{t-1}, y_q^{t-1}, \hat{y}^{t-1}) \quad (6)$$

Here, we use s_q^t to denote the EV market share on path q in the t_{th} time period, the variable ε to denote the constant natural growth of market share, and initial EV market share for each path s_q^0 is given. We use variable y_q^{t-1} to denote the EV flow coverage on path q in $t - 1_{th}$ time period and variable \hat{y}^{t-1} to denote the average flow coverage in the whole network in the $t - 1_{th}$ time period. Here, y_q^{t-1} is a continuous variable on $[0, 1]$ denoting the percentage proportion of the EV flow demand covered.

We define the relationship of EV market share between time periods as follows:

$$s_q^t = (1 + w_1\varepsilon + w_2(y_q^{t-1} - \hat{y}^{t-1}))s_q^{t-1} \quad (7)$$

Here, the constant w_i , $i \in \{1, 2\}$ are the coefficient for different variables, denoting the weight for the general charging opportunity and path specific charging opportunity with summation of 1. On the right side of equal sign, we have the natural growth of market share ε as one of the major factors that affect the current EV market share s_q^t (general charging opportunity). For this part, all the paths in the network will be equally changed as we assume the natural growth of market share in the whole network is the same. The other major factor would be the path flow coverage difference in the previous time period $y_q^{t-1} - \hat{y}^{t-1}$ (path specific charging opportunity). We assume that higher coverage in the path will stimulate EV market share growth, while lower coverage in the path will cause the potential decrease in EV market share. We define our market share with the assumption of people's decision of buying EVs will be mainly related to the infrastructures on the shortest path of their origin and destination. This assumption helps simplify our problem while travelers might travel between multiple O-D pairs with the same vehicle. However, people's purchasing decisions might be related to other facts according to previous studies. Hong and Kuby (2016) assume that drivers living in a given zone will not purchase an AFV until the refueling infrastructure can successfully satisfy a certain threshold percentage of their travel demand. Also, household with multiple vehicles could make different choices on purchasing EVs (Tamor and Milačić, 2015; Hidrue et al., 2011). Zheng et al. (2012) also mention that HOV lane and parking space access are available to EV users in several states in the US in order to promote EV purchase. With our assumption, the EV market share growth will be different on each path, relating with the flow coverage on that path. With different weight constants, we could provide different demand dynamics scenarios. Thus, the decisions on the location of stations as well as the number of modules installed will affect the future market share on each path indirectly. We summarize demand dynamics of two scenarios as follows.

Scenario 1. *General charging opportunity.* Higher weight of w_1 . Natural market growth is the major factor in demand dynamic, and users' decision is less affected by flow coverage.

Scenario 2. *Path specific charging opportunity.* Higher weight of w_2 . Flow on each path is the major factor in demand dynamic, and users' decision is mainly affected by flow coverage.

Several other demand dynamics that are less realistic than our definition of the changing of EV market share are also listed.

Alternative 1: $s_q^t = \varepsilon + s_q^{t-1}$

Alternative 2: $s_q^t = w_1\varepsilon + w_2s_q^{t-1} + w_3y_q^{t-1} + w_4\hat{y}^{t-1} + w_5$

Alternative 3: $s_q^t = w_1s_q^{t-1}\varepsilon + w_2y_q^{t-1} + w_3\hat{y}_q^{t-1} + w_4$

In Alternative 1, this is the basic case where the EV market share increases by a constant independent of infrastructure or market share in earlier time periods. The second alternative assume a linear relationship between all factors that will affect the market share with different weights, providing an enhanced scenario of Alternative 1. Since the unit of market share, natural growth and flow coverage are different and we have limited information about the correlation of these variables, the summation we have in Alternative 2 could provide us with less realistic results in numerical experiments due to poor choices of weight coefficients. Similarly for alternative 3, we need more accurate estimations of weight coefficients to have realistic results while we can set weight coefficients as percentage value in our definition in (7) due to its special form. With equation (7), we set the EV market share in the earlier time period as the basic value, natural growth and flow coverage will affect the basic value as factors in percentage. Then, we can easily apply different values in factor weights w_1, w_2 satisfying the constraint $w_1 + w_2 = 1$ to observe the performance of different market scenarios. The results of numerical experiments are shown in the later sections.

3.3 Formulation of the Multi-period Capacitated AC-PC Model

The Multi-period Capacitated AC-PC model (MCACPC) extends the AC-PC model of Capar et al. (2013), and additionally considers the capacity limit of stations, the multi-period planning and demand dynamics. We impose constraints of the total number of charged vehicles at each charging station by the number of modules while maximizing the total flow coverage, and the EV flow is related to market share in each time period. In later sections, an objective function of maximizing the market share in the next time period is also discussed.

Using the notation given in Table 3, we provide the following formulation:

$$\max \sum_{t \in T} \sum_{q \in Q} s_q^t f_q^0 y_q^t \quad (8)$$

subject to:

$$\sum_{i \in K_{jk}^q} z_i^t \geq y_q^t \quad \forall q \in Q, a_{jk} \in A^q, t \in T \quad (9)$$

$$\sum_{q \in Q} e_q g_{qi} s_q^t f_q^0 y_q^t \leq c x_i^t + M(1 - z_i^t) \quad \forall i \in N, t \in T \quad (10)$$

$$s_q^t = (1 + w_1\varepsilon + w_2(y_q^{t-1} - \hat{y}^{t-1}))s_q^{t-1} \quad \forall q \in Q, t \in T \quad (11)$$

$$x_i^t \leq M z_i^t \quad \forall i \in N, t \in T \quad (12)$$

$$\sum_{i \in N} (\alpha_i z_i^t + \beta_i x_i^t) \leq B^t \quad \forall t \in T \quad (13)$$

Table 3: Notation for the Multi-period Capacitated AC-PC (8)–(18)

T	Set for all time periods
N	Set for all the nodes in the network
Q	Set for all the paths in the network
A^q	Set for all adjacent arcs on path q
K_{jk}^q	Set of candidate nodes for arc from j to k on path q
f_q^0	Initial demand of path q
s_q^0	Initial EV market share of path q
e_q	Constant used to adjust the short trips within vehicle range
g_{qi}	Number of charging times on path q at node i
c	Capacity of each module
M	Constant large enough
α_i	Cost of building a station at site i
β_i	Cost of building one module at site i
B^t	Cumulative budget available till the t -th time period
ε	Natural growth of EV market share
y_q^t	Linear variable, the flow coverage rate on path q in the t -th time period
\hat{y}^t	Linear variable, the average flow coverage rate in the network in the t -th time period
z_i^t	Binary variable, whether a station is built at site i in the t -th time period
x_i^t	Integer variable, the number of modules built at site i in the t -th time period
s_q^t	Linear variable, market share of EV on path q in the t -th time period

$$z_i^t \leq z_i^{t+1} \quad \forall i \in N, t \in T \quad (14)$$

$$x_i^t \leq x_i^{t+1} \quad \forall i \in N, t \in T \quad (15)$$

$$0 \leq y_q^t \leq 1 \quad \forall q \in Q, t \in T \quad (16)$$

$$z_i^t \in \{0, 1\} \quad \forall i \in N, t \in T \quad (17)$$

$$x_i^t \in \{\text{nonnegative integers}\} \quad \forall i \in N, t \in T \quad (18)$$

The objective function (8) is to maximize the total flow covered in all time periods. Constraint (9) is similar as the original AC-PC model, which makes sure that the locations we choose covers the path. Constraint (10) is the main constraint for capacity on each station. Here, we define e_q as

$$\frac{1}{\max(1, \lceil \frac{\text{range}}{\text{roundtrip distance}} \rceil)}$$

to denote the fraction of round trips that require charging on average in path q , and $\lceil \cdot \rceil$ means rounding to the nearest integer. We take value of g_{qi} as 2 if node i is not the origin or destination

of path q , meaning the vehicle must stop at the station to charge in both directions, as 1 if node i is the origin or destination of path q since the vehicle will stop to charge in either one direction and as 0 if node i is not on path q . We use c to denote the capacity of each module. These definitions of coefficients are consistent with the definitions in CFRLM from Upchurch et al. (2009). For constraint (10), the RHS limit the station capacity by its module number while LHS stands for the average total number of vehicle stops that may take place in the location. Suppose there is not a station built in location i in time period t , we would easily have $z_i^t = 0$ as well as $x_i^t = 0$. Then RHS of constraint (10) would be the large constant M , meaning that the amount of flow passing through this node i is not limited and no vehicle will stop to recharge at this location. On the other hand, suppose we do have an open station $z_i^t = 1$ and a number of modules $x_i^t > 0$, the amount of flow passing through this node i will be limited by the RHS of the constraint with value cx_i^t which is the capacity of the open facility. In addition, our constraint (10) is different from the constraint (5) in CFRLM which does not include the big M . Although the idea that the flow passing through a node with no open facility will not be limited are the same for two constraints, the constraint (5) in CFRLM has different definitions of coefficient g_{qhk} since the variable value is pre-decided for each path q , each combination h and each location k . For a location k with no open facility, we will have $g_{qhk} = 0$ for k not in combination h that can refuel path q and y_{qh} is not limited even though we have $x_k = 0$ on the RHS. Thus, the constraint (5) holds for the condition when flow can pass through a node on the path with no open facility freely. For our constraint (10) without combination information, we might have location i with no open facility on path q where $g_{qi} > 0$ and $z_i = 0, x_i = 0$. Thus, we need $M(1 - z_i)$ to make sure that the flow on path q is not limited by the zero capacity on RHS since no vehicle need to charge at this location. Constraint (11) is based on the idea of demand dynamics, relating the present market share to the flow coverage and market share in the past. We adapt different weight coefficients w_1, w_2 to show the diverse scenarios of demand dynamics. Constraint (12) makes sure that modules would only be built at locations that are identified as stations. Constraint (13) limit the budge based on station and module construction cost. Here, the constant α_i denotes the cost of building a charging station at location i and the constant β_i denotes the cost of installing one unit of module at location i , then constraint (13) will make sure the total cost of building stations and installing modules will be within the budget for the current time period. Constraints (14) and (15) make sure that all the stations or modules built in earlier time periods still exist in the later time periods.

We can also substitute the objective function with

$$\max \sum_{t \in T} \sum_{q \in Q} s_q^t f_q^0 \quad (19)$$

to maximize the total EV market share in the network for all time periods.

The proposed formulation of Multi-Period Capacitated AC-PC model will try to solve the problem for all time periods, giving us an optimal solution. Even if it may not reach the maximum flow coverage in each single time period, the total flow coverage would be maximized.

4 Solution Methods

The Multi-period Capacitated AC-PC model becomes significantly more complicated than the original AC-PC model since it includes nonlinear objective function and nonlinear constraints. For small networks, it can be solved directly with MINLP solver, for example Bonmin (2016) solver in short amount of time. For larger networks, the computation time increases exponentially in the CPLEX solver to close the gap between upper bounds and lower bounds even for single-period capacitated problems, and obtaining an optimal solution is rarely possible. To balance the solution quality and computational time, we present a heuristic method to solve the problem: the Forward Method. This myopic method will return a single time period solution based on the optimal solution of the previous time period in each iteration, which does not guarantee a global optimal solution to our original MCACPC problem.

We can sketch the heuristic method as follows:

1. Solve the Single-period Capacitated AC-PC model for the current time period (planning time period).
2. Decide the charging station locations and the number of modules to be placed in each station for the current time period.
3. Move to the next time period, and update the Single-period Capacitated AC-PC model for the current time period based on the charging station location and module number from the previous time period.
4. Repeat this process until the last time period.

The Forward Method starts the computation from the first planning time period, and the number of chargers and modules increases with time period updating. This would be similar to infrastructure planning in reality.

4.1 The Forward Method

In the Forward Method, we first solve a Single-period Capacitated AC-PC model for the first time period and obtain the location of charging stations as well as the number of modules built in each site. In the next time period, we will make sure that the number of modules at all sites are larger than those of the earlier time period. We will repeat this process until we obtain a final optimal solution in the last time period.

At the beginning of time period t , we know the value of the location variables z^{t-1} , the number of modules variables x^{t-1} as well as s^{t-1} from the previous time period $t-1$. Easily, we can calculate the s_q for the current time period t with equation (7). For the initial time period, we let $z^0 = 0$ and $x^0 = 0$, or any existing charging locations and number of existing modules. For time period t , we

have the available budget B_t . For each time period t , we solve the following problem:

$$\max_{x,y,z} \sum_{q \in Q} s_q f_q^0 y_q \quad (20)$$

subject to:

$$\sum_{i \in K_{jk}^q} z_i \geq y_q \quad \forall q \in Q, a_{jk} \in A^q \quad (21)$$

$$\sum_{q \in Q} e_q g_{qi} s_q f_q^0 y_q \leq c x_i + M(1 - z_i) \quad \forall i \in N \quad (22)$$

$$x_i \leq M z_i \quad \forall i \in N \quad (23)$$

$$\sum_{i \in N} (\alpha_i z_i + \beta_i x_i) \leq B_t \quad (24)$$

$$z_i \geq z_i^{t-1} \quad \forall i \in N \quad (25)$$

$$x_i \geq x_i^{t-1} \quad \forall i \in N \quad (26)$$

$$0 \leq y_q \leq 1 \quad \forall q \in Q \quad (27)$$

$$z_i \in \{0, 1\} \quad \forall i \in N \quad (28)$$

$$x_i \in \{\text{nonnegative integers}\} \quad \forall i \in N \quad (29)$$

Then we call the solutions z^t and x^t , and proceed to the next time period until the final time period.

As we can see, this is a model for a specific time period. The difference between models in different time periods lies in constraints (25) and (26) to ensure that previously installed charging stations and modules are continued to be used.

4.1.1 Two-Phase Approach in Each Time Period

Solving a Single-period capacitated AC-PC model (20)–(29) in the Forward Method can still be time-consuming if the network scale is large. We propose a two-phase approach to help improve computational time for solving the single-period capacitated AC-PC model (20)–(29).

Our two phase heuristic method is developed based on the decomposition of the original MCACPC model. The main idea is to separate the decision-making of location z and number of modules x for each time period t . The first step is to solve an AC-PC problem to find the location of stations in order to maximize the total flow coverage in time period t . Given the locations of stations from Step 1, the second step determines the number of modules to be built in each station so as to maximize the total flow coverage.

Since we cannot determine the optimal number of stations to be built in each time period *a priori*, we enumerate all possible cases of the number of stations, denoted by p_t for time period t . The smallest possible value of p_t is $\sum_{i \in N} z_i^{t-1}$, and the largest possible value of p_t is $\min(\lfloor \frac{B_t}{\min_{i \in N} (\alpha_i + \beta_i)} \rfloor, |N|)$, where $\lfloor x \rfloor$ means the largest integer value that is no greater than x and $|X|$ means the number of

elements in set X . For the cases when the number of p_t values to examine is large, we will later discuss how to avoid the full enumeration in Section 4.2.

For *each* value of p within the range of p_t , we solve two problems: the first-phase problem to determine z and the second-phase problem to determine x . Given the location decision vector z^{t-1} , the first-phase problem determines locations of charging stations.

(Phase 1 model)

$$\max_{z,y} \sum_{q \in Q} s_q f_q^0 y_q \quad (30)$$

subject to

$$\sum_{i \in K_{jk}^q} z_i \geq y_q \quad \forall q \in Q, a_{jk} \in A^q \quad (31)$$

$$\sum_{i \in N} z_i = p \quad (32)$$

$$z_i \geq z_i^{t-1} \quad \forall i \in N \quad (33)$$

$$y_q \in \{0, 1\} \quad \forall q \in Q \quad (34)$$

$$z_i \in \{0, 1\} \quad \forall i \in N \quad (35)$$

Note that the above problem is an instance of the AC-PC problem proposed by Capar et al. (2013). Let $z^t(p)$ denote the solution obtained for the given p_t . Given the location solution $z^t(p)$ and the number of existing chargers x^{t-1} , we solve the following second phase problem:

(Phase 2 model)

$$\phi_t(p) = \max_{x,y} \sum_{q \in Q} s_q f_q^0 y_q \quad (36)$$

subject to

$$\sum_{i \in K_{jk}^q} z_i^t(p) \geq y_q \quad \forall q \in Q, a_{jk} \in A^q \quad (37)$$

$$\sum_{q \in Q} e_q g_{qi} s_q f_q^0 z_i^t(p) y_q \leq c x_i \quad \forall i \in N \quad (38)$$

$$x_i \leq M z_i^t(p) \quad \forall i \in N \quad (39)$$

$$\sum_{i \in N} (\alpha_i z_i^t(p) + \beta_i x_i) \leq B^t \quad (40)$$

$$x_i \geq x_i^{t-1} \quad \forall i \in N \quad (41)$$

$$0 \leq y_q \leq 1 \quad \forall q \in Q \quad (42)$$

$$x_i \in \{\text{nonnegative integers}\} \quad \forall i \in N, t \in T \quad (43)$$

Then we use vector x^t to denote the solution obtained. Note that the big M in (39) may be replaced by $\frac{B^t - \alpha_i}{\beta_i}$, which is the smallest constant that serves the purpose of constraint (39).

After we compute $\phi_t(p)$, i.e. the optimal objective function value of the second-phase problem, for each p from $\sum_{i \in N} z_i^{t-1}$ to $\min(\lfloor \frac{B_t}{\min_{i \in N}(\alpha_i + \beta_i)} \rfloor, |N|)$, we choose the largest $\phi_t(p)$ and let the corresponding p value be p_t . Finally, we obtain the corresponding z^t and x^t vectors as optimal solutions to the time period t problem in the Forward Method (20)–(29).

4.1.2 Revising the Second-Phase Model

During our experiments, we found that optimization solvers like CPLEX tend to install unnecessary modules while solving the second-phase model (36)–(43) (as we explained in the simple example in Appendix A). To break the tie among alternative optimal solutions as we would like, we suggest to replace the objective function in (36) as follows:

(Revised Phase 2 model)

$$\max_{x,y} \sum_{q \in Q} s_q f_q^0 y_q - \gamma \sum_{i \in N} x_i \quad (44)$$

$$\text{subject to} \quad (37)–(43) \quad (45)$$

where γ is a small positive constant. We will still use $\sum_{q \in Q} s_q f_q^0 y_q$ as the value of $\phi_t(p)$ at the optimality.

The constant γ needs to be carefully chosen. We propose the γ value as in the following lemma:

Lemma 1. Suppose p is a fixed positive integer and $z^t(p)$ is an optimal solution to the first-phase problem (30)–(35). Let (\bar{x}, \bar{y}) and (\hat{x}, \hat{y}) be solutions to the second-phase problem (36)–(43) and the revised second-phase problem (44)–(45), respectively. If we choose

$$\gamma = \frac{\eta}{100} \frac{\beta}{\Gamma} \sum_{q \in Q} s_q f_q^0, \quad (46)$$

where

$$\Gamma = B_t - \sum_{i \in N} \alpha_i z_i^t(p) \quad \text{and} \quad \beta = \min_{i \in N} \beta_i,$$

then we have

$$\sum_{q \in Q} s_q f_q^0 \bar{y}_q - \sum_{q \in Q} s_q f_q^0 \hat{y}_q \leq \frac{\eta}{100} \sum_{q \in Q} s_q f_q^0. \quad (47)$$

That is, the loss of flow coverage in the revised second-phase problem is bounded by $\eta\%$ of the total flow.

Proof. See Appendix B. □

Choosing a smaller value of η results in a smaller loss of possible flow coverage in the revised second-phase problem, which provides a better choice of charger locations and module number.

4.1.3 Summary of the Forward Method

We summarize the Forward Method as follows:

Step 0. Initialization. Let z^0 and x^0 be zero vectors. Set $t = 1$.

Step 1. Searching p_t . For each value of p from $\sum_{i \in N} z_i^{t-1}$ to $\min(\lfloor \frac{B_t}{\min_{i \in N}(\alpha_i + \beta_i)} \rfloor, |N|)$, do the following:

Step 1(a). Solving the First-phase Problem. Given z^{t-1} , s_q^{t-1} and p , solve (30)–(35), and call the solution $z^t(p)$.

Step 1(b). Solving the Second-phase Problem. Given $z^t(p)$, x^{t-1} and s_q^{t-1} , solve (44)–(45), and call the solution $x^t(p)$ and $y^t(p)$. Let $\phi_t(p) = \sum_{q \in Q} s_q f_q^0 y_q^t(p)$.

Step 2. Determining p_t . Among all $\phi_t(p)$ values computed, we take the largest value and let $x^t = x^t(p)$, $y^t = y^t(p)$, $z^t = z^t(p)$, and $p^t = p$ for the corresponding p value.

Step 3. Updating s_q^t . With the $y^t = y^t(p)$ computed in the current time period and the s_q^{t-1} from the last time period, update the s_q^t value with equation (7).

Step 4. Termination. If $t = |T|$, stop; otherwise, update $t \leftarrow t + 1$ and go to Step 1.

Since the market share s_q^t is related to s_q^{t-1} and flow coverage in the last time period, we can successfully apply the Forward Method on our original model with demand dynamics. However, the backward method will not work as it requires pre-generation of EV market share in the final time period without knowing the EV demand in the earlier time periods.

4.2 Line Search Method

While the two-phase approach can reduce the computational time for solving the single time-period problems, we still need to enumerate all possible p values. This can be computationally inefficient for large-scale problems. A possible solution is to use a line search method such as the Golden Section search (Kiefer, 1953). Although it is not proved to be quasi-convex, our numerical experiments indicate that $\phi_t(p)$ is nearly quasi-convex. While a line search method is generally guaranteed to converge to an optimal solution for strictly quasi-convex functions (Bazaraa et al., 2013), we propose to use a line search method for searching p that maximizes $\phi_t(p)$ for each time period p .

The original Golden Section method can only be applied on continuous functions. We slightly modify the Golden Section method to find the optimal p value that needs to be integers, and hence discrete. We also allow a full enumeration within the final interval of pre-set length l to reduce changes of finding a sub-optimal solution.

Initialization Step Choose an allowable final length of uncertainty $l > 0$, l is integer. Let a_1 and b_1 be the smallest and largest possible values of p , respectively. Let $\lambda_1 = \lfloor a_1 + (1 - \alpha)(b_1 - a_1) \rfloor$ and $\mu_1 = \lfloor a_1 + \alpha(b_1 - a_1) \rfloor$, where $\alpha = 0.618$. Evaluate $\phi_t(\lambda_1)$ and $\phi_t(\mu_1)$, let $k = 1$, and go to Main Step.

- Main Steps**
1. If $b_k - a_k \leq l$, stop; the optimal solution is either a_k or b_k with the greater ϕ_t function value. Otherwise, if $\phi_t(\lambda_k) \leq \phi_t(\mu_k)$, go to Step 2; and if $\phi_t(\lambda_k) > \phi_t(\mu_k)$, go to Step 3.
 2. Let $a_{k+1} = \lambda_k$ and $b_{k+1} = b_k$. Furthermore, let $\lambda_{k+1} = \mu_k$, and let $\mu_{k+1} = \lfloor a_{k+1} + \alpha(b_{k+1} - a_{k+1}) \rfloor$. Evaluate $\phi_t(\mu_{k+1})$ and go to Step 4.
 3. Let $a_{k+1} = a_k$ and $b_{k+1} = \mu_k$. Furthermore, let $\mu_{k+1} = \lambda_k$, and let $\lambda_{k+1} = \lfloor a_{k+1} + (1 - \alpha)(b_{k+1} - a_{k+1}) \rfloor$. Evaluate $\phi_t(\lambda_{k+1})$ and go to Step 4.
 4. Replace k by $k + 1$ and go to Step 1.

Final Step Perform a full enumeration in the final interval with uncertainty of length l to find an optimal solution.

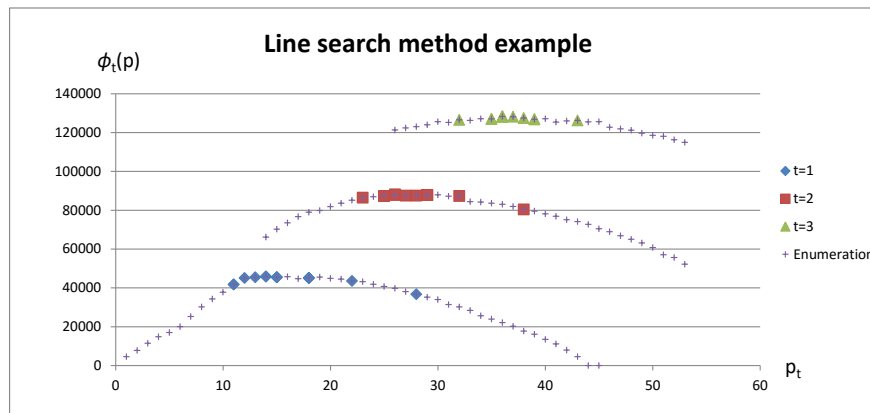


Figure 1: An example comparing line search method and the original enumeration method

Figure 1 provides the results from the line search method. We apply the line search method to quickly locate the peak positions, and then use a full enumeration to find the exact peak value. This process can reduce the computational time significantly. For the example in Figure 1, a full enumeration for all three time periods requires checking 113 cases while line search method only considers 23 cases for the multi-period planning, thus greatly reducing the computation time.

As the line search method does not guarantee an optimal solution for $\phi_t(p)$, the above line search method indeed obtains sub-optimal solutions in some cases. Our numerical experiments indicate that the gap between the full enumeration result and the line search result is usually within 5 to 10 percent. While we lose the optimality in searching p , we certainly gain reduction in the computation time, which is 113 fully enumerated cases to 24 searches in the example presented in Figure 1.

5 Case Study

In the following section, we utilize the Sioux-Falls test network (LeBlanc et al., 1975; Li et al., 2016) to compare the computational performance of different solution methods of multi-period capacitated

AC-PC model. Later, we provide numerical results based on US Northeastern network to analyze the trend of EV market share as well as charging availability under different demand dynamics scenarios.

5.1 Sioux Falls Network

We apply the multi-period capacitated model on the Sioux Falls Network, which is a popular test network for transportation analysis. See Figure 2.

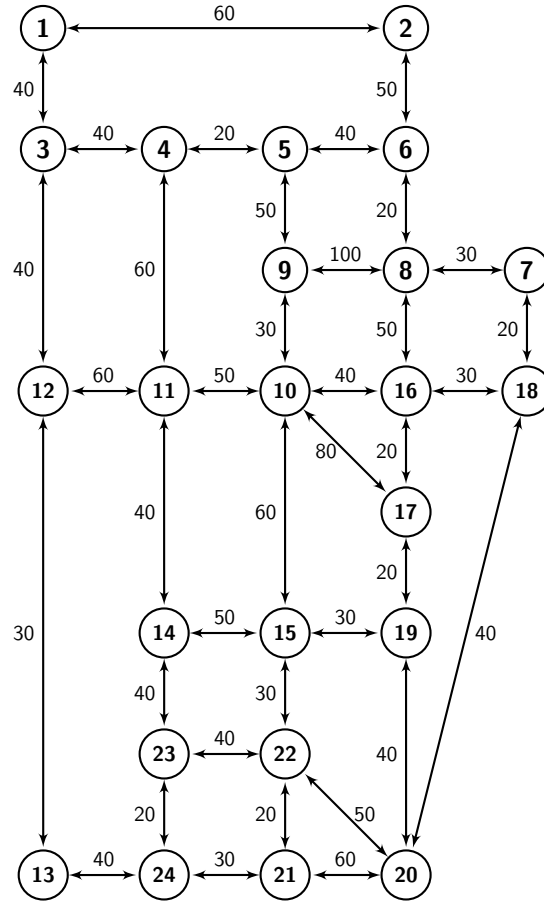


Figure 2: Sioux Falls network

The Sioux Falls network has 24 nodes and 38 undirected arcs (76 directed arcs). Node index is labeled in the circle of each node, and the link length is labeled near the arc with unit of miles. Charging stations can be built in any of the 24 nodes while several nodes are chosen as OD pairs as scenarios of different problem size. We assume that the EV market share of all paths for the first time period is 10% and the natural growth rate is set as 20%. For example, market share will increase to 12% in the second time period. And the demand dynamics coefficients are set as $w_1 = 0.05$ and $w_2 = 0.95$ to emphasis user's decision. The construction cost for each EV charging station in a new location is \$45K and each module for the station would cost \$22.5K (Agenbroad and Holland, 2014). Here, we use 1K to denote 1000. Each module can serve 48 vehicles as capacity.

The budget in different time periods considering different number of OD pairs are listed in Table 4, making sure the flow coverage in the network is neither too low or too high. The range of vehicles are set as 100 miles. The flow demand between OD pairs are randomly generated.

Budget	$t = 1$	$t = 2$	$t = 3$
$N = 4$	200	250	300
$N = 8$	600	750	900
$N = 12$	1,000	1,250	1,500
$N = 16$	500	1,500	2,500
$N = 20$	500	1,500	2,500
$N = 24$	500	1,500	2,500

Table 4: Sioux Falls network budget in unit of \$1K

$T = 2$

Number of OD pairs	MINLP solution	Forward solution	Solution gap	MINLP CPU time	Forward CPU time
$N = 4$	14.61	14.61	0.00%	302.37	3.90
$N = 8$	834.10	781.28	6.33%	102.83	3.86
$N = 12$	1270.90*	1270.90	0.00%	3610.92	4.78
$N = 16$	1345.79*	1377.31	2.34%	7222.78	8.36
$N = 20$	1432.19*	1397.87	2.40%	7210.71	4.39
$N = 24$	1439.67*	1399.47	2.79%	10824.19	12.73

*Not solved to optimality

Table 5: Computational results for two time periods. CPU times are in seconds.

$T = 3$

Number of OD pairs	MINLP solution	Forward solution	Solution gap	MINLP CPU time	Forward CPU time
$N = 4$	34.42	34.42	0.00%	318.00	3.58
$N = 8$	1561.07	1401.28	10.24%	114.95	3.88
$N = 12$	2295.94*	2279.27	0.73%	3612.95	4.01
$N = 16$	NA	3234.58	NA	7222.78	4.50
$N = 20$	NA	3340.77	NA	7441.61	6.08
$N = 24$	NA	3351.65	NA	11364.14	11.89

*Not solved to optimality

Table 6: Computational results for three time periods. CPU times are in seconds.

We apply the MCACPC model with various infrastructure planning time periods, and implement our model in the Julia language using the JuMP package (Lubin and Dunning, 2015). To solve

the mixed integer nonlinear programming (MINLP) problem in (8)–(18) we used the Bonmin (2016) solver. We used CPLEX to solve MIP subproblems in Forward Method. The computational performance is shown in Table 5 and 6 for two time periods and three time periods cases. We run the MINLP solver to solve different cases with various number of OD pairs, and feasible solution labeled with (*) is provided when optimal solution is not found within given computational time. We use NA to denote the cases where the MINLP solver failed to provide feasible solution within given computational time. We limit the computational time for the MINLP solver for $N = 12$ case to 3600s, $N = 16$ or 20 cases to 7200s and $N = 24$ case to 10800s considering the problem size. The total CPU times are slightly larger than those limits, because pre-processing and optimization model generation times are included. The solution gap is calculated by the difference between the solution of two methods divided by the MINLP solution. As we can see in the computational results, the difference between the MINLP solver solutions and the Forward Method solutions is quite small and the maximum gap between two solutions is around 10%. However, we can see the computational time for Forward method is far less than that of MINLP solver. For some cases where we have more OD pairs and time periods, the MINLP solver could not even find a feasible solution within hours. We could infer that Forward method performs well while balancing the solution quality and computational time, and the advantages of Forward method would be more obvious when dealing with larger networks consisting of more OD pairs where MINLP solver would failed to provide solutions due to problem size. Numerical results based on larger random networks are shown in Appendix C.

5.2 DC-NY-BOS Network

We apply the multi-period capacitated model on the US Northeast region, covering Washington DC, New York and Boston (DC-NY-BOS Network). See Figure 3. The network, created with QGIS (2015), is based on US primary road shapefile from Tigerline (2015) as well as the highway network on Bing Maps (2015). We obtain a network with 317 nodes and 510 undirected arcs (1020 directed arcs), and these nodes are potential sites for us to build charging stations and modules. The 123 red nodes are OD nodes, and the corresponding zones are the demand source for each OD node. We collect the total population in each zone, and these are the population weight for each corresponding OD node for each zone. We also generate the demand matrix based on a gravity spatial interaction model (Fotheringham and OKelly 1989):

$$OD_{ij} = cP_iP_j/d_{ij}^2$$

where OD_{ij} is the total flow demand f_q from site i to site j (q is the index of the path from i to j), c is a scale constant, P_i , P_j are the population at site i , j , and d_{ij} is the distance between OD pairs. Thus, we are able to get a demand matrix with total traffic flow on each OD pair. Only paths longer than the vehicle range are considered in the case study.

We make several assumptions in this case study of DC-NY-BOS Network:

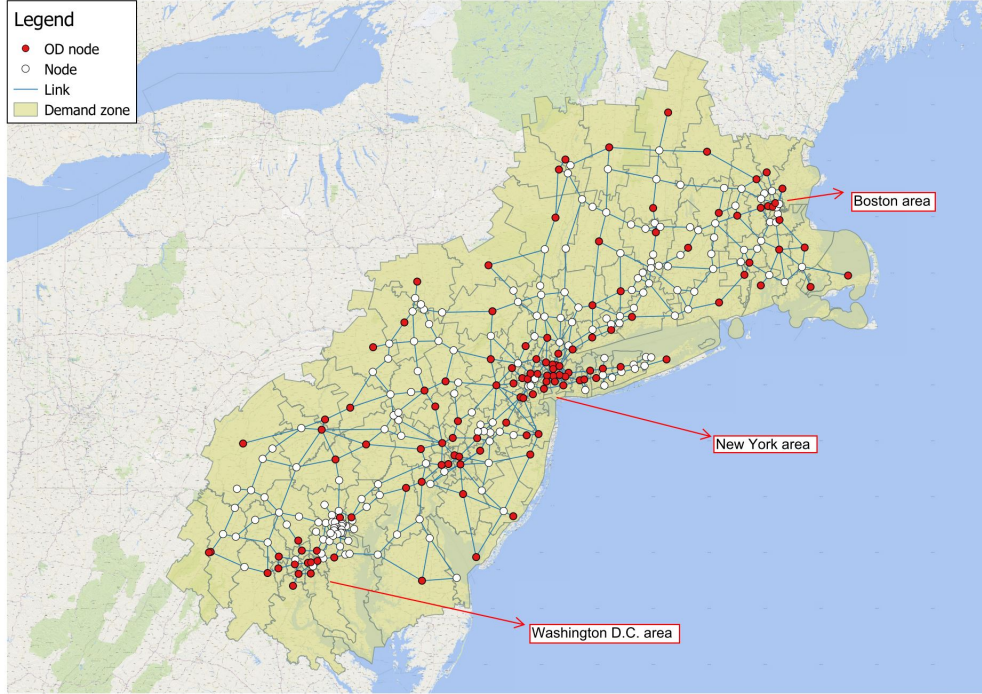


Figure 3: DC-NY-BOS Network

1. All links are two-directional freeways;
2. The length of each time period is one year;
3. EV demand in all paths increases naturally with a fixed rate by each time period;
4. Only tier-3 charging (DC) stations are considered;
5. Each module takes 30 minutes to charge one EV to full battery and it will serve one EV at a time;
6. All EVs have a range of 80 miles.

We solve the multi-period capacitated model with three infrastructure planning time periods applying the Forward Method, and implement our model in Julia (Lubin and Dunning, 2015) with CPLEX solver. As we are building the charging network for EVs, we only consider the EV market share of the total traffic flow. We assume that the EV market share of all paths for the first time period is 1.4% and the market share will increase by 0.3 % per time period (Yang, 2014). However, we have not included demand dynamics and we only consider the trivial natural growth of the market here. The construction cost for each EV charging station in a new location is \$45K and each module for the station would cost \$22.5K (Agenbrood and Holland, 2014). The three-time period planning budget is \$2500K for the first, \$5000K for the second and \$7500K for the last time period. The capacity constant c is 48 given assumption 4.

5.2.1 Demand Dynamics in Three Time Periods

In the following case study, we test two scenarios of demand dynamics based on the Forward method. The first scenario, related to general charging opportunities, assumes that natural growth of the EV demand would have a major impact on the EV market share in the network, taking $w_1 = 0.95, w_2 = 0.05$ in equation (7). The second scenario with different coefficients $w_1 = 0.05, w_2 = 0.95$, which is sensitive to path specific, assumes the major impact is from the EV flow coverage on each path. We use subscript to denote the result of time period $i \in \{1, 2, 3\}$.

We can have a more detailed view of the distribution of stations and modules on the link coverage graph with the former model results under diverse demand dynamics. From the total flow covered and EV market share for each path, we can calculate the total EV flow as well as the covered EV flow going through each link. We use different colors to show the rate of coverage in the network, and squares of different size to show the number of modules. We also present the 123 OD nodes in our network with 317 nodes.

We define the total flow covered (TFC) on link i :

$$TFC_i = \sum_{q \in Q} s_q f_q y_q \delta_q^i \quad (48)$$

then easily have the flow coverage rate (FCR) on link i :

$$FCR_i = \frac{\sum_{q \in Q} s_q f_q y_q \delta_q^i}{\sum_{q \in Q} s_q f_q \delta_q^i} \quad (49)$$

where the set Q contains all of the paths, and $\delta_q^i = 1$ if node i is on the path q and $\delta_q^i = 0$ otherwise.

We can see most of the flow focus on a primary corridor connecting DC, New York and Boston, and some branches extend to nearby areas in Figure 4.

Here, Figure 5 provide the results of two different scenarios based on three construction time periods with the Forward Method. Arcs with deeper color has higher flow coverage rate, while larger square on nodes denote more modules at that location. Each figure shows the flow coverage rate on each path in the current time period, and we use t to denote the t -th time period. We can observe a major difference between two scenarios in the covered area of the whole network in Figure 5. In scenario 1, most of the stations and modules distribute on the primary corridor of the network while some stations with smaller number of modules are located in suburban area, covering more area of the network. However, almost all stations and modules are built to satisfy the need on the primary corridor and very limited flow on the other parts of the network is covered in scenario 2. Considering the property of two scenarios, it is not difficult to conclude that we have a more average growth of EV demand in scenario 1, which leads to a network with more covered area. On the other hand, the facilities tend to focus on satisfying area with higher demands in scenario 2, which leads to a network with only primary corridor well covered.

However, when we focus on the total flow covered in the network for both scenarios as shown in



Figure 4: Initial total flow on each link

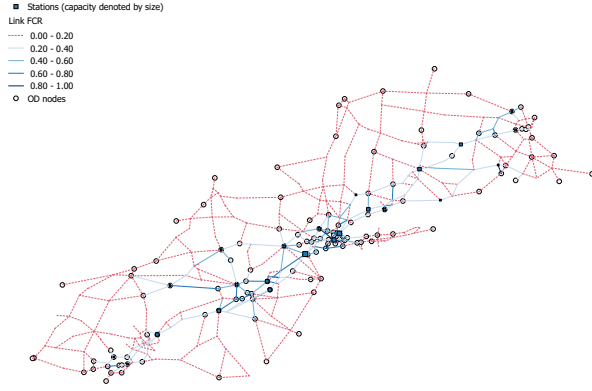
Figure 6, we can see that most of the covered flow are along the primary corridor, and the flow in other area are much less. The difference between two scenarios are less obvious than that in FCR figures.

We also visualize the average market share on each link i which is similar to FCR in Figure 7, in order to show the different properties of two scenarios.

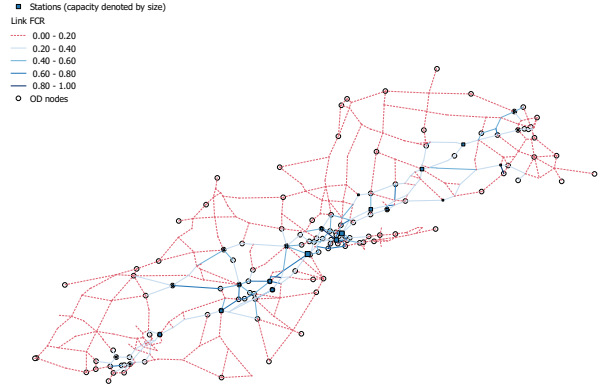
In Figure 7, we visualize the market share difference in the third time period and the second time period $\Delta s_q = s_q^3 - s_q^2$ in the network. Blue links show positive difference indicating the EV market share grows, and red links show negative difference indicating the market share decreases. As we can see, the EV market share in the network shows an average growth in scenario 1, while only the primary corridor has positive growth and the market share in other parts of the network is decreasing in scenario 2. Thus, we can conclude that demand dynamics in scenario 2 can surely provide a higher coverage rate of 91% in the whole network comparing that of 78% in scenario 1, while it is not helping EV users in urban area and we will see the potential disadvantage in later experiments.

5.2.2 Potential Problems in Multi-Period Planning for Different Demand Dynamics

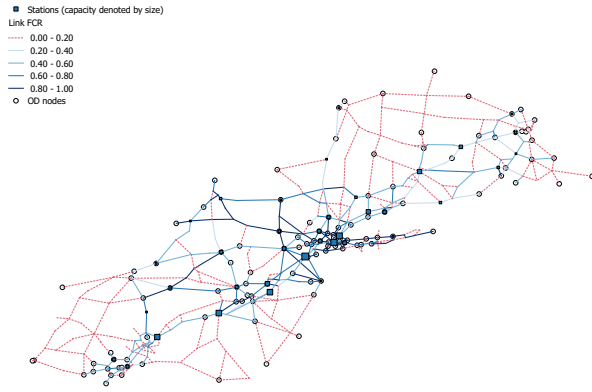
The purpose of multi-planning of charging network is to provide fundamental facilities for EV users, in order to attract more EV users and improve EV market share. However, as we can see in scenario 2, the coverage rate for the network is higher while the market share decreases in most part of the network. The decreasing of the market share reduces the flow in the network, which leads to



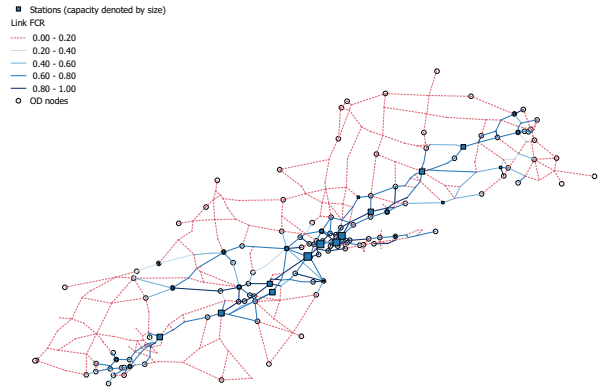
(a) Scenario 1, link FCR, $t = 1$



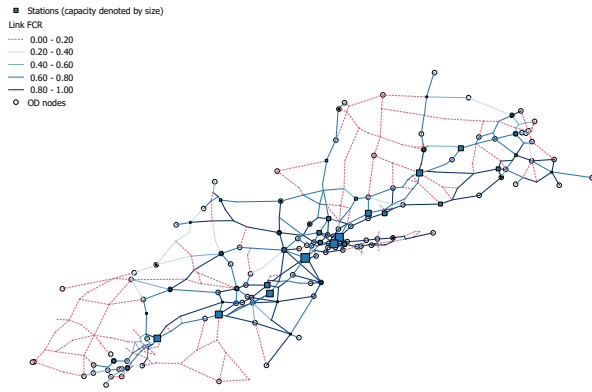
(b) Scenario 2, link FCR, $t = 1$



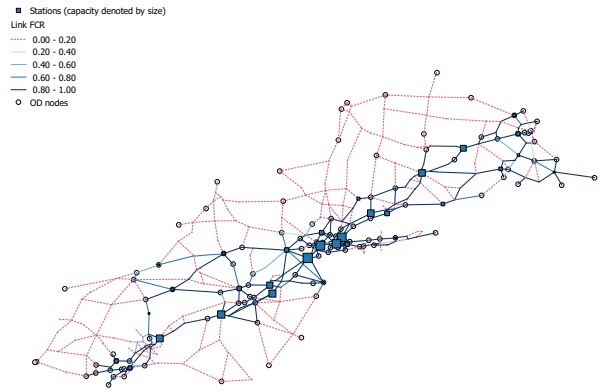
(c) Scenario 1, link FCR, $t = 2$



(d) Scenario 2, link FCR, $t = 2$



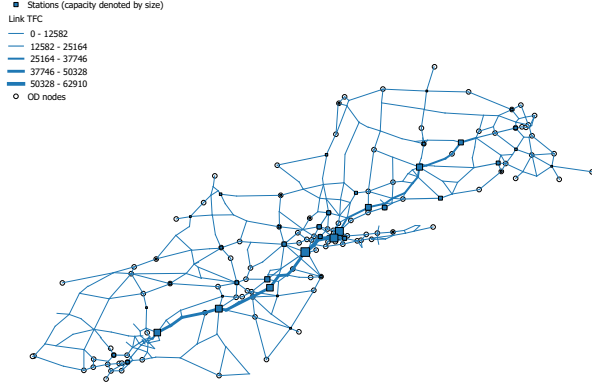
(e) Scenario 1, Average link FCR=78%, $t = 3$



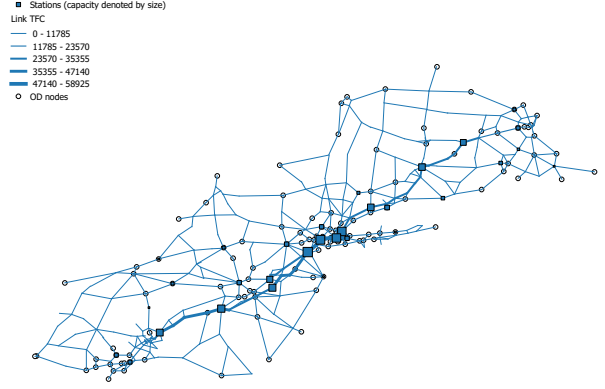
(f) Scenario 2, Average link FCR=91%, $t = 3$

Figure 5: Flow coverage rate on DC-NY-BOS network in each time period

higher coverage rate and lower covered flow in scenario 2. Even though the total EV market share is increasing, this fact is conflict with the purpose of attracting EV users and improve EV market share, which could be a potential problem for the charging network.

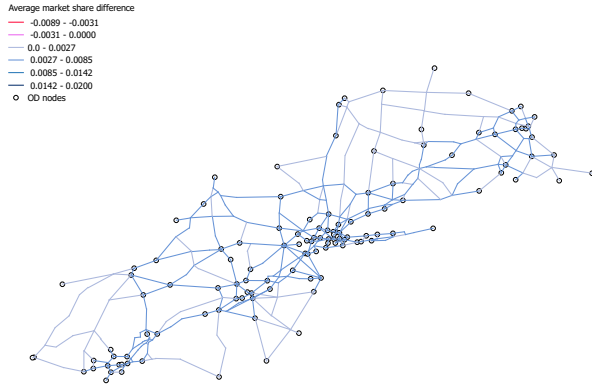


(a) Scenario 1, link TFC, $t = 3$

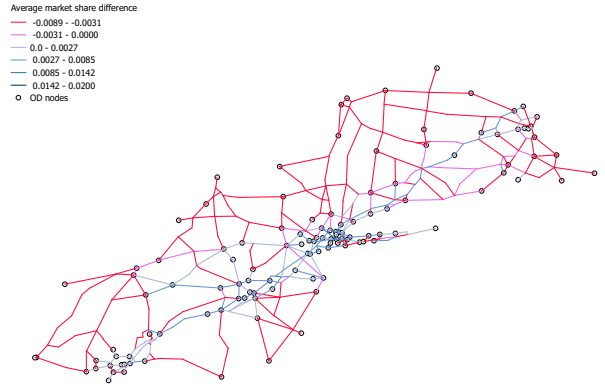


(b) Scenario 2, link TFC, $t = 3$

Figure 6: Total flow covered on DC-NY-BOS network



(a) Scenario 1, Market share, $t = 3$



(b) Scenario 2, Market share, $t = 3$

Figure 7: Market share on DC-NY-BOS network

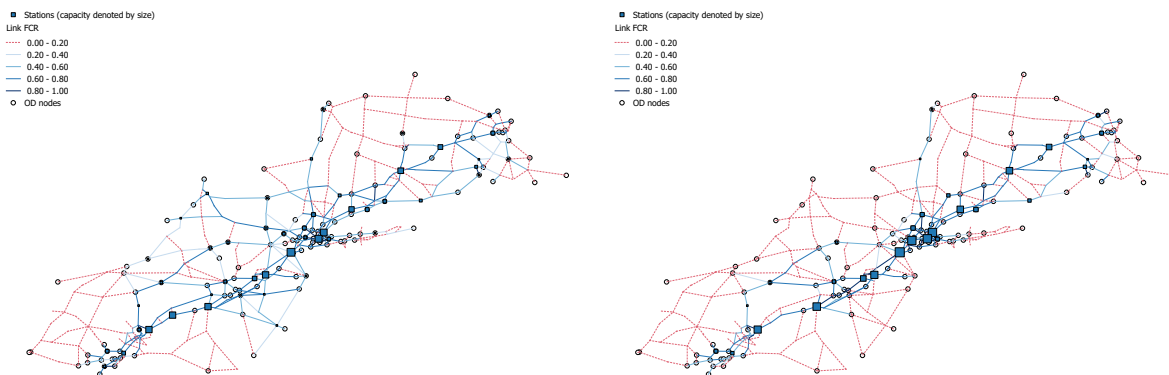
In order to avoid this situation of higher coverage and lower total flow, one of the possible solutions is to change the objective function from maximizing the flow covered to maximizing the market share in the next time period. Thus, we can modify the objective to $\max \sum_{q \in Q} s_q^t f_q^0$ in Forward Method. Since the demand dynamics equation (7) in the form of $s_q^t = (1 + w_1 \varepsilon + w_2 (y_q^{t-1} - \hat{y}^{t-1})) s_q^{t-1}$ was used in our original problem, the objective function would become constant while solving the problem with Forward Method. While by changing the equation to $s_q^t = (1 + w_1 \varepsilon + w_2 (y_q^t - \hat{y}^t)) s_q^{t-1}$, we can maximize the EV market share in the next time period, and y^t would appear as a variable instead of a constant from the last period in the Forward Method. The result are shown in Table 7. In this table, we show the summation of EV flow on all paths in the network as *Total EV flow*, the summation of covered EV flow on all paths in the network as *Covered EV flow* and the average proportion of all covered flow in the total flow as *Coverage rate*. We use *msd* to denote the EV market share difference between the last time period and the first time period.

Table 7: Numerical results for different objectives

Objective function	Max covered flow		Max market share	
	Scenario 1, $t = 3$	Scenario 2, $t = 3$	Scenario 1, $t = 3$	Scenario 2, $t = 3$
Total EV flow	190669.89	183179.42	193917.01	240154.09
Covered EV flow	149314.73	167111.69	119641.51	171905.01
Coverage rate	0.7831	0.9123	0.617	0.7158
Average msd	0.00583	0.00229	0.00583	0.00316
Max msd	0.006771	0.02002	0.007304	0.03418
Min msd	0.0051	-0.00887	0.005612	-0.00235

As we can see in Table 7, we observe much higher total EV flow in the network while maximizing the EV market share flow. However, the cost is the total coverage rate, which decrease by around 10%. Also, we can see that results based on scenario 1 provides a higher average market share, while the total number of EV is smaller than that in scenario 2. With this new objective, it is possible for us to construct a charging network that satisfy the need of either coverage rate or total EV flow better. With different objective functions, our model is flexible to diverse needs of policy makers.

Here are the flow coverage rate figures in Figure 8 and the market share figures in Figure 9 for both scenarios with modified objective function in the 3rd time period.



(a) Scenario 1, link FCR

(b) Scenario 2, link FCR

Figure 8: Flow coverage rate based on Max market share on DC-NY-BOS network

We can still observe significant differences on the flow coverage in two scenarios, which is similar as the phenomena in Figures 5e and 5f. As we can see in Figures 8a and 8b, more stations are built in different locations in scenario 1 while more modules are installed in fewer locations in scenario 2. In addition, the market share growth in both scenarios in Figure 9 is less than that in Figure 7 since our objective is to maximize the total EV flow. We can observe more obvious difference of market share growth for different objectives in scenario 2. According to the definition of our demand dynamics,

$$s_q^t = (1 + w_1\varepsilon + w_2(y_q^{t-1} - \hat{y}^{t-1}))s_q^{t-1}$$

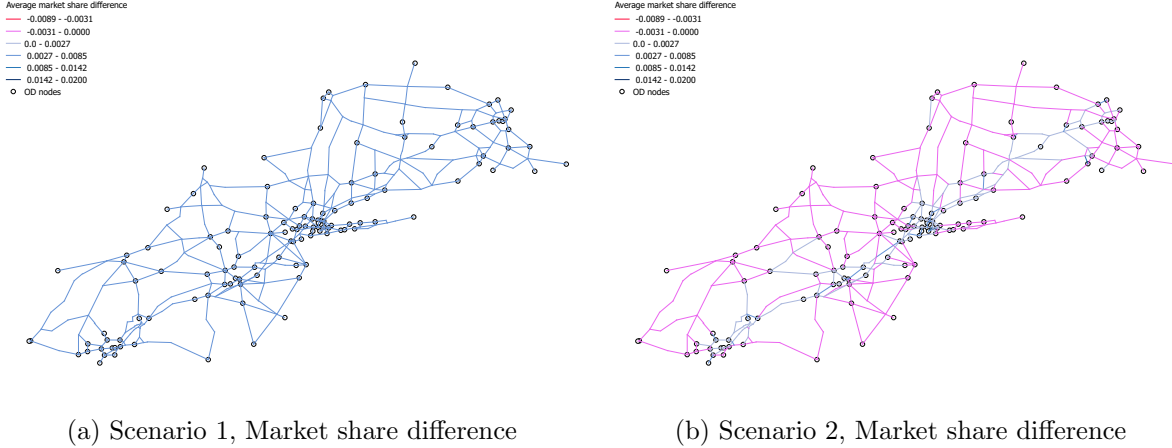


Figure 9: Market share changing based on Max market share on DC-NY-BOS network

the EV market share s_q^t on paths with higher flow coverage ($y_q^{t-1} - \hat{y}^{t-1} \geq 0$) will keep increasing in future time periods, while the EV market share s_q^t on paths with lower flow coverage or uncovered ($y_q^{t-1} - \hat{y}^{t-1} \leq 0$) will keep decreasing in future time periods. Thus, we can see the distribution of stations and modules as well as EV market share are quite different for two scenarios since each scenario has different coefficients for diverse factors. This will lead to the fact that installing more modules on existing stations will increase EV market share, and the growing EV flow needs more modules to satisfy the demand. Thus, less new stations will be built and less area are covered in the whole network.

5.2.3 Numerical Results based on Longer Time Periods

The former experiments are based on 3 time periods to simplify the process of computing, while we also present the results for longer time periods.

The following results are based on the existing two scenarios as well as the two objectives for 8 time periods, and the natural growth would be 0.3% for each time period while the budget increases equally from \$500K to \$7500K. We use *maximizing EV flow covered* to denote the case where we maximize the total flow covered in the objective function, while *maximizing EV flow* denotes the case where we maximize the total flow in the network.

In Figure 10a, we observe decreasing after time period 5, which is quite different from the 3-time-period result with increasing coverage rate. By checking the total flow in Figure 10b, we see the exponential growth of EV flow for scenario 2 while the budget grows in a linear way. Then, the investment of charging facilities cannot satisfy the fast growing demand, which causes the coverage of the network to decrease in longer time periods. Since the total flow grows slowly at first, the coverage rate of the network will keep increasing in earlier time periods. We can also observe the trade-off between coverage rate and total flow in Figure 10 since MaxCover has higher coverage rate and lower total flow while MaxDemand has higher total flow and lower coverage rate.

In Figure 11, we can observe decreasing in scenario 2 dynamics after a sharp increase of coverage

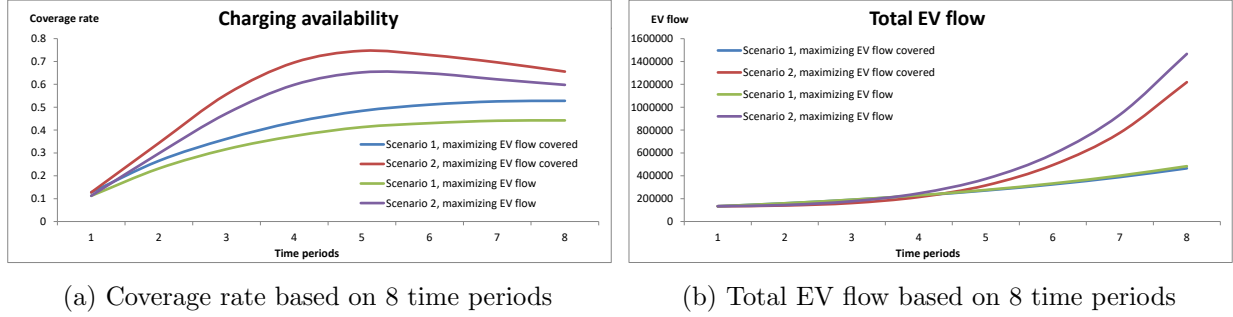


Figure 10: Numerical results based on 8 time periods

rate, while there is little increase in the total flow. Also, we can observe much higher total EV flow if we aim to maximize the EV market share instead of the flow coverage.

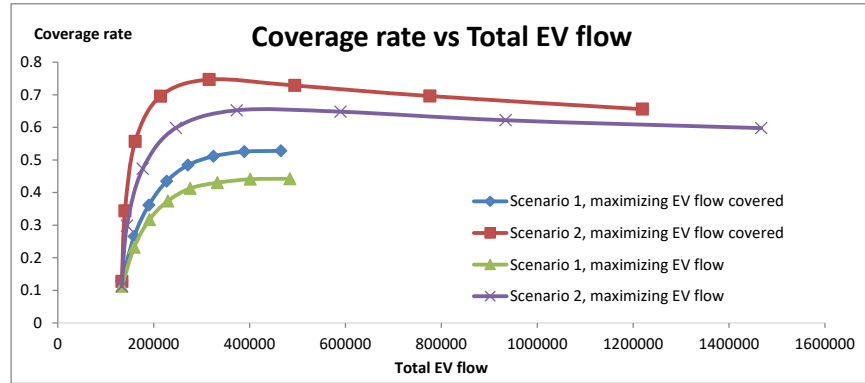


Figure 11: Comparing coverage rate and total EV flow in all scenarios

We also provide numerical results on the number of modules in each potential location of the network for all time periods in Figure 12, where we can observe the actual different solutions for our diverse demand dynamics and objective function scenarios. Locations with significantly more modules is shown in scenario 2, while more stations with fewer number of modules can be observed in scenario 1. Also, the solutions for different model objectives with same demand dynamics are quite similar. In scenario 1, user's decision would have less effect on EV market share, and EV market share will mainly increase by the natural growth rate. In scenario 2, more modules helps improve EV market share and the increasing EV flow requires more modules at the same location, which results in less stations in the network. This is consistent with the conclusion of our 3 time period model results that less area are covered in scenario 2.

6 Conclusion and Future Research

Previous studies have focused on the initial infrastructure planning while EVs and charging stations has appeared on the market for several years. Station capacity helps to provide more realistic results, and multi-period planning should also be considered as it follows the regular pattern of

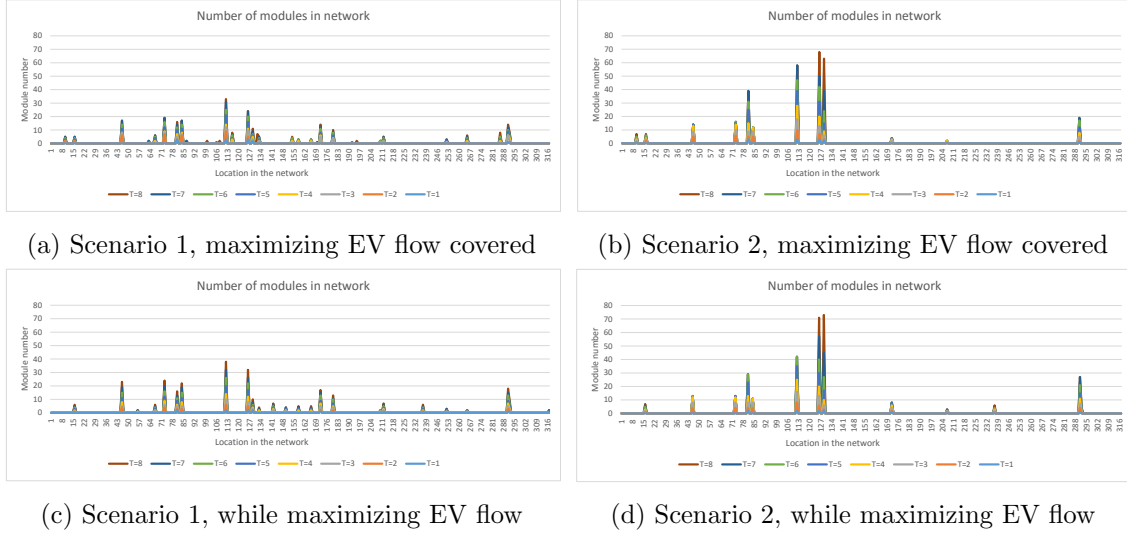


Figure 12: Numerical results on module number in network in each time period

facility construction in real life. According to our case study, demand dynamics, serving as the interaction between network users and network planners, would have much impact on the distribution of charging stations as the EV market keep growing in future time periods. Thus, new models considering the growth of EV market and existing charging facilities would be useful to provide more realistic planning results.

In this paper, we have studied the multi-period planning of the charger location problem for EVs with considerations of facility capacity and demand dynamics. We provide a new formulation of flow refueling location problem, which will help us determine the locations of chargers as well as the number of charging modules at each station over multiple time periods. Based on the idea of covering each arc on the path, the new formulation maximizes the total flow covered with the flow going through each node being limited. As the new formulation is computationally difficult to solve for optimal results for large networks, we present a heuristic method to solve the model. In addition, we use a line search method to improve computational time for the heuristic method. We also provide a flexible equation to test diverse dynamic scenarios that simulate the growing of EV market share in reality, which helps reveal the potential problems in our multi-period planning model.

A case study based on Sioux Falls Network is introduced to test the computational performance of our heuristic method, and another case study based on the Washington D.C. to Boston (DC-NY-BOS) network is performed to provide numerical results on different demand dynamic scenarios and model objectives. Link coverage and market share growth of the network are visualized to indicate the infrastructure planning decision discrepancy as well as potential disadvantage, and the flexible objective function could also affect planning decisions. Observations in longer time period are also shown for both demand scenarios and model objectives.

Based on the results of our case study, we are able to present the following suggestions for policy

makers.

1. Multi-period planning model tends to satisfy the need of centralized high demand area if EV market share is closely related to facility construction, while more area in the network will be covered if EV demand growth is independent of facility construction.
2. Focusing on the total flow coverage of the network could result in low EV market share in most area of the network under specific demand dynamics in reality, which is less friendly to some EV users.
3. The trade-off between EV demand growth and network flow coverage can be adjusted with different planning objective.
4. The charging availability might decrease after long time period in current planning model with path specific sensitive demand, due to the insufficient budget comparing to the rapidly increasing EV demand.
5. Planning decisions could be greatly affected by the diverse demand dynamics, while planning objective is less important.

This paper provides an ample potential for further study. Our facility capacity is defined as the number of vehicles that could be served in unit time. New assumptions concerning the charging strategy could be included to provide a more realistic model, including stochastic charging time and queuing time at each charging station.

Demand forecast could be a direction of the future research. We are assuming the EV market share will follow simple rules for the whole network. More realistic demand forecast methods considering driver's decision and network property might help provide more accurate planning models.

References

- Agenbrood, J., B. Holland. 2014. EV Charging Station Infrastructure Costs. Rocky Mountain Institute. URL http://blog.rmi.org/blog_2014_04_29_pulling_back_the_veil_on_ev_charging_station_costs.
- Ahn, J., G. Jeong, Y. Kim. 2008. A forecast of household ownership and use of alternative fuel vehicles: A multiple discrete-continuous choice approach. *Energy Economics* **30**(5) 2091–2104.
- Arslan, O., O. E. Karaşan. 2016. A Benders decomposition approach for the charging station location problem with plug-in hybrid electric vehicles. *Transportation Research Part B: Methodological* **93** 670–695.
- Bazaraa, M. S., H. D. Sherali, C. M. Shetty. 2013. *Nonlinear programming: theory and algorithms*. John Wiley & Sons.

- Berman, O., R. C. Larson, N. Fouska. 1992. Optimal location of discretionary service facilities. *Transportation Science* **26**(3) 201–211.
- Bing Maps. 2015. Map <https://www.bing.com/maps/>.
- Bonmin. 2016. Basic Open-source Nonlinear Mixed INteger programming <https://projects.coin-or.org/Bonmin>.
- Boyacı, B., K. G. Zografos, N. Geroliminis. 2017. An integrated optimization-simulation framework for vehicle and personnel relocations of electric carsharing systems with reservations. *Transportation Research Part B: Methodological* **95** 214–237.
- Brownstone, D., D. S. Bunch, T. F. Golob, W. Ren. 1996. A transactions choice model for forecasting demand for alternative-fuel vehicles. *Research in Transportation Economics* **4** 87–129.
- Capar, I., M. Kuby. 2012. An efficient formulation of the flow refueling location model for alternative-fuel stations. *IIE Transactions* **44**(8) 622–636.
- Capar, I., M. Kuby, V. J. Leon, Y.-J. Tsai. 2013. An arc cover–path-cover formulation and strategic analysis of alternative-fuel station locations. *European Journal of Operational Research* **227**(1) 142–151.
- Chen, Z., F. He, Y. Yin. 2016. Optimal deployment of charging lanes for electric vehicles in transportation networks. *Transportation Research Part B: Methodological* **91** 344–365.
- Chung, S. H., C. Kwon. 2015. Multi-period planning for electric car charging station locations: A case of korean expressways. *European Journal of Operational Research* **242**(2) 677–687.
- Dagsvik, J. K., T. Wennemo, D. G. Wetterwald, R. Aaberge. 2002. Potential demand for alternative fuel vehicles. *Transportation Research Part B: Methodological* **36**(4) 361–384.
- Davis, P., T. Ray. 1969. A branch-bound algorithm for the capacitated facilities location problem. *Naval Research Logistics Quarterly* **16**(3) 331–344.
- Drezner, Z. 1984. The p -centre problem—heuristic and optimal algorithms. *Journal of the Operational Research Society* **35**(8) 741–748.
- Ewing, G., E. Sarigöllü. 2000. Assessing consumer preferences for clean-fuel vehicles: A discrete choice experiment. *Journal of Public Policy & Marketing* **19**(1) 106–118.
- Fetene, G. M., G. Hirte, S. Kaplan, C. G. Prato, S. Tsharaktschiew. 2016. The economics of workplace charging. *Transportation Research Part B: Methodological* **88** 93–118.
- Hakimi, S. L. 1964. Optimum locations of switching centers and the absolute centers and medians of a graph. *Operations Research* **12**(3) 450–459.

- Hakimi, S. L. 1965. Optimum distribution of switching centers in a communication network and some related graph theoretic problems. *Operations Research* **13**(3) 462–475.
- Hidrué, M. K., G. R. Parsons, W. Kempton, M. P. Gardner. 2011. Willingness to pay for electric vehicles and their attributes. *Resource and Energy Economics* **33**(3) 686–705.
- Hodgson, M. J. 1990. A flow-capturing location-allocation model. *Geographical Analysis* **22**(3) 270–279.
- Hof, J., M. Schneider, D. Goeke. 2017. Solving the battery swap station location-routing problem with capacitated electric vehicles using an avns algorithm for vehicle-routing problems with intermediate stops. *Transportation Research Part B: Methodological* **97** 102–112.
- Hong, S., M. Kuby. 2016. A threshold covering flow-based location model to build a critical mass of alternative-fuel stations. *Journal of Transport Geography* **56** 128–137.
- Kiefer, J. 1953. Sequential minimax search for a maximum. *Proceedings of the American Mathematical Society* **4**(3) 502–506.
- Kuby, M., S. Lim. 2005. The flow-refueling location problem for alternative-fuel vehicles. *Socio-Economic Planning Sciences* **39**(2) 125–145.
- Kuby, M., S. Lim. 2007. Location of alternative-fuel stations using the flow-refueling location model and dispersion of candidate sites on arcs. *Networks and Spatial Economics* **7**(2) 129–152.
- LeBlanc, L. J., E. K. Morlok, W. P. Pierskalla. 1975. An efficient approach to solving the road network equilibrium traffic assignment problem. *Transportation Research* **9**(5) 309–318.
- Li, S., Y. Huang, S. J. Mason. 2016. A multi-period optimization model for the deployment of public electric vehicle charging stations on network. *Transportation Research Part C: Emerging Technologies* **65** 128–143.
- Liao, C.-S., S.-H. Lu, Z.-J. M. Shen. 2016. The electric vehicle touring problem. *Transportation Research Part B: Methodological* **86** 163–180.
- Lim, S., M. Kuby. 2010. Heuristic algorithms for siting alternative-fuel stations using the flow-refueling location model. *European Journal of Operational Research* **204**(1) 51–61.
- Liu, C., D. L. Greene. 2012. Consumer vehicle choice model documentation. Tech. rep., Oak Ridge National Laboratory (ORNL), Oak Ridge, TN (United States).
- Liu, H., D. Z. Wang. 2017. Locating multiple types of charging facilities for battery electric vehicles. *Transportation Research Part B: Methodological* .
- Lubin, M., I. Dunning. 2015. Computing in Operations Research Using Julia. *INFORMS Journal on Computing* **27**(2) 238–248. doi: 10.1287/ijoc.2014.0623. URL <http://dx.doi.org/10.1287/ijoc.2014.0623>.

- Melaina, M., J. Bremson. 2008. Refueling availability for alternative fuel vehicle markets: sufficient urban station coverage. *Energy Policy* **36**(8) 3233–3241.
- Melaina, M. W. 2003. Initiating hydrogen infrastructures: preliminary analysis of a sufficient number of initial hydrogen stations in the us. *International Journal of Hydrogen Energy* **28**(7) 743–755.
- Minieka, E. 1970. The m -center problem. *SIAM Review* **12**(1) 138–139.
- MirHassani, S., R. Ebrazi. 2012. A flexible reformulation of the refueling station location problem. *Transportation Science* **47**(4) 617–628.
- Montoya, A., C. Guéret, J. E. Mendoza, J. G. Villegas. 2017. The electric vehicle routing problem with nonlinear charging function. *Transportation Research Part B: Methodological* .
- Nicholas, M. A., J. Ogden. 2006. Detailed analysis of urban station siting for california hydrogen highway network. *Transportation Research Record: Journal of the Transportation Research Board* **1983**(1) 121–128.
- Nie, Y. M., M. Ghamami, A. Zockaie, F. Xiao. 2016. Optimization of incentive polices for plug-in electric vehicles. *Transportation Research Part B: Methodological* **84** 103–123.
- QGIS. 2015. A Free and Open Source Geographic Information System <http://www.qgis.org/en/site/>.
- Romm, J. 2006. The car and fuel of the future. *Energy Policy* **34**(17) 2609–2614.
- Sa, G. 1969. Branch-and-bound and approximate solutions to the capacitated plant-location problem. *Operations Research* **17**(6) 1005–1016.
- Schwoon, M. 2007. A tool to optimize the initial distribution of hydrogen filling stations. *Transportation Research Part D: Transport and Environment* **12**(2) 70–82.
- Shukla, A., J. Pekny, V. Venkatasubramanian. 2011. An optimization framework for cost effective design of refueling station infrastructure for alternative fuel vehicles. *Computers & Chemical Engineering* **35**(8) 1431–1438.
- Stephan, C., J. Sullivan. 2004. An agent-based hydrogen vehicle/infrastructure model. *Evolutionary Computation, 2004. CEC2004. Congress on*, vol. 2. IEEE, 1774–1779.
- Strehler, M., S. Merting, C. Schwan. 2017. Energy-efficient shortest routes for electric and hybrid vehicles. *Transportation Research Part B: Methodological* .
- Suzuki, A., Z. Drezner. 1996. The p -center location problem in an area. *Location Science* **4**(1) 69–82.
- Tamor, M. A., M. Milačić. 2015. Electric vehicles in multi-vehicle households. *Transportation Research Part C: Emerging Technologies* **56** 52–60.

- Tigerline. 2015. Geography, US Census Bureau <https://www.census.gov/geo/maps-data/data/tiger-line.html>.
- Toregas, C., R. Swain, C. ReVelle, L. Bergman. 1971. The location of emergency service facilities. *Operations Research* **19**(6) 1363–1373.
- Upchurch, C., M. Kuby, S. Lim. 2009. A model for location of capacitated alternative-fuel stations. *Geographical Analysis* **41**(1) 85–106.
- Wang, Y.-W., C.-C. Lin. 2009. Locating road-vehicle refueling stations. *Transportation Research Part E: Logistics and Transportation Review* **45**(5) 821–829.
- Wang, Y.-W., C.-C. Lin. 2013. Locating multiple types of recharging stations for battery-powered electric vehicle transport. *Transportation Research Part E: Logistics and Transportation Review* **58** 76–87.
- Wang, Y.-W., C.-R. Wang. 2010. Locating passenger vehicle refueling stations. *Transportation Research Part E: Logistics and Transportation Review* **46**(5) 791–801.
- Xu, M., Q. Meng, K. Liu. 2017a. Network user equilibrium problems for the mixed battery electric vehicles and gasoline vehicles subject to battery swapping stations and road grade constraints. *Transportation Research Part B: Methodological* **99** 138–166.
- Xu, M., Q. Meng, K. Liu, T. Yamamoto. 2017b. Joint charging mode and location choice model for battery electric vehicle users. *Transportation Research Part B: Methodological* .
- Yang, Z. 2014. Electric vehicle markets have their ups and downs (2014 YTD update). The International Council of Clean Transportation. URL <http://www.theicct.org/blogs/staff/electric-vehicle-markets-have-their-ups-and-downs-2014-ytd-update>.
- Zeng, W., I. Castillo, M. J. Hodgson. 2010. A generalized model for locating facilities on a network with flow-based demand. *Networks and Spatial Economics* **10**(4) 579–611.
- Zheng, J., S. Mehndiratta, J. Y. Guo, Z. Liu. 2012. Strategic policies and demonstration program of electric vehicle in china. *Transport Policy* **19**(1) 17–25.

Appendix

A Simple example on alternative solution in the revised second-phase model

Let us consider a simple example here. Suppose we have a 4-node network as follows in Figure 13 where arc length is labeled near each link. Suppose we have vehicle range as 10, station construction

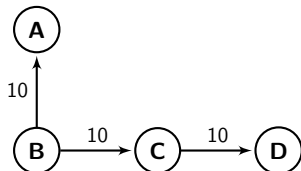


Figure 13: Simple network example

cost as 40, module construction cost as 20, the amount of EV flow from node B to node A is 5 and the amount of EV flow from node B to node D is 5. If the capacity of each module is 5 and the budget for the first time period is 80, we can easily reach the conclusion that the optimal solution is to build at node B and at least one module is needed to satisfy the demand from B to A . In order to satisfy the EV flow from B to D , we need another charging station at node C in addition to the open facility at node B . However, we do not have enough budget for a new station and new modules at node C and one module is enough to consider the flow from B to A . Suppose we have budget of 120 for the second time period, it should be enough to satisfy all demands in the network since we can install two stations and one module for each station. While we have budget of 80 in the first time period, we can choose to install one module or two modules at location B and the optimal objective function for the current time period will be the same. If we choose to install two stations at node B , we would not have enough budget to install modules at new station at node C since we only have additional budget of 40. Thus, we can see alternative optimal solutions in the previous time period do affect optimal objective function value in the following time periods. In order to eliminate this suboptimal condition, we should only install necessary modules to satisfy the demand and save the budget of unnecessary modules for future use.

B Proof

Proof of Lemma 1. From (40), we have

$$\sum_{i \in N} \beta_i \bar{x}_i \leq B_t - \sum_{i \in N} \alpha_i z_i^t(p).$$

Let $\beta = \min_{i \in N} \beta_i$. Then, we have

$$\sum_{i \in N} \bar{x}_i \leq \frac{B_t - \sum_{i \in N} \alpha_i z_i^t(p)}{\beta}$$

Since $\sum_{i \in N} \hat{x}_i \geq 0$, we obtain

$$\sum_{i \in N} \bar{x}_i - \sum_{i \in N} \hat{x}_i \leq \frac{B_t - \sum_{i \in N} \alpha_i z_i^t(p)}{\beta} \quad (50)$$

By definition, we know that

$$\sum_{q \in Q} s_q f_q^0 \bar{y}_q \geq \sum_{q \in Q} s_q f_q^0 \hat{y}_q$$

and

$$\sum_{q \in Q} s_q f_q^0 \bar{y}_q - \gamma \sum_{i \in N} \bar{x}_i \leq \sum_{q \in Q} s_q f_q^0 \hat{y}_q - \gamma \sum_{i \in N} \hat{x}_i.$$

Combining these two inequalities, we obtain

$$0 \leq \sum_{q \in Q} s_q f_q^0 \bar{y}_q - \sum_{q \in Q} s_q f_q^0 \hat{y}_q \leq \gamma \left(\sum_{i \in N} \bar{x}_i - \sum_{i \in N} \hat{x}_i \right) \leq \gamma \frac{B_t - \sum_{i \in N} \alpha_i z_i^t(p)}{\beta}$$

where we used (50). With the choice of γ in (46), we obtain

$$\sum_{q \in Q} s_q f_q^0 \bar{y}_q - \sum_{q \in Q} s_q f_q^0 \hat{y}_q \leq \frac{\eta}{100} \sum_{q \in Q} s_q f_q^0,$$

which completes the proof. \square

C Computational results based on random networks

We present the computational results based on random networks in order to test our method with larger size problems. We generate random networks with similar method as that provided by Capar et al. (2013). We randomly generate n nodes in a $[0, 1000]^2$ coordinate system, and the distance between each node is defined as the Euclidean distance. We connect all nodes with the minimum spanning tree, and add n shortest edges in addition to the MST. Then we choose m nodes out of n as the OD nodes. We also randomly generate the population of each OD node, and use the gravity model to estimate the total flow between an OD pair. We present the results in Table 8.

Note that the actual solving time ranges significantly depending on the capacity, path flow as well as budget settings. We install large number of stations and modules to reach appropriate flow coverage (around 40% to 90%) since parameter estimation is difficult. The computational time can be greatly reduced if more detailed number of stations and modules are given during the construction planning.

Table 8: Numerical results for random networks

Forward method (CPU time in seconds)			
Number of nodes	200		
Number of OD nodes	30	60	120
CPU solving time	26.40	125.47	5953.96
Number of stations built	43	30	42
Number of modules built	133	273	562
Number of nodes	500		
Number of OD nodes	30	60	120
CPU solving time	114.71	1857.72	392818.78
Number of stations built	80	82	230
Number of modules built	173	504	1764
Number of nodes	1000		
Number of OD nodes	30	60	120
CPU solving time	5641.94	40629.46	>432000*
Number of stations built	235	183	NA
Number of modules built	861	967	NA

*Terminated due to long computational time